Medium-Chain Acyl-Coenzyme A Dehydrogenase Bound to a Product Analogue, Hexadienoyl-Coenzyme A: Effects on Reduction Potential, pK_a, and Polarization†

Jackson D. Pellett,‡ Kim Marie Sabaj,‡ Avery W. Stephens,‡ Alasdair F. Bell,§ Jiaquan Wu,§ Peter J. Tonge,§ and Marian T. Stankovich*,‡

Department of Chemistry, University of Minnesota, 207 Pleasant Street SE, Kolthoff and Smith Halls, Minneapolis, Minnesota 55455, and Department of Chemistry, State University of New York, Stony Brook, New York 11794-3400

Received March 21, 2000; Revised Manuscript Received August 11, 2000

ABSTRACT: 2,4-Hexadienoyl-coenzyme A (HD-CoA) has been used to investigate the redox and ionization properties of medium-chain acyl-CoA dehydrogenase (MCAD) from pig kidney. HD-CoA is a thermodynamically stabilized product analogue that binds tightly to oxidized MCAD ($K_{dox} = 3.5 \pm 0.1$ μM, pH 7.6) and elicits a redox potential shift that is 78% of that observed with the natural substrate/product couple [Lenn, N. D., Stankovich, M. T., and Liu, H. (1990) *Biochemistry 29*, 3709−3715]. The midpoint potential of the MCAD·HD-CoA complex exhibits a pH dependence that is consistent with the redox-linked ionization of two key glutamic acids as well as the flavin adenine dinucleotide (FAD) cofactor. The estimated ionization constants for Glu376-COOH (p$K_{a,ox} \approx 9.3$) and Glu99-COOH (p$K_{a,ox} \approx 7.4$) in the oxidized MCAD·HD-CoA complex indicate that while binding of the C_6 analogue makes Glu376 a stronger catalytic base (p$K_{a,ox} \approx 6.5$, free MCAD), it has little effect on the pK of Glu99 (p$K_{a,ox} \approx 7.5$, free MCAD) [Mancini-Samuelson, G. J., Kieweg, V., Sabaj, K. M., Ghisla, S., and Stankovich, M. T. (1998) *Biochemistry 37*, 14605−14612]. This finding is in agreement with the apparent pK of 9.2 determined for Glu376 in the human MCAD·4-thia-octenoyl-CoA complex [Rudik, I., Ghisla, S., and Thorpe, C. (1998) *Biochemistry 37*, 8437−8445]. The pK_as estimated for Glu376 and Glu99 in the reduced pig kidney MCAD·HD-CoA complex, 9.8 and 8.6, respectively, suggest that both of these residues remain protonated in the charge-transfer complex under physiological conditions. Polarization of HD-CoA in the enzyme active site may contribute to the observed pK_a and redox potential shifts. Consequently, the electronic structures of the product analogue in its free and MCAD-bound forms have been characterized by Raman difference spectroscopy. Binding to either the oxidized or reduced enzyme results in localized π-electron polarization of the hexadienoyl C(1)═O and C(2)═C(3) bonds. The C(4)═C(5) bond, in contrast, is relatively unaffected by binding. These results suggest that, upon binding to MCAD, HD-CoA is selectively polarized such that partial positive charge develops at the C(3)−H region of the ligand, regardless of the oxidation state of the enzyme.

Fatty acid acyl-CoA dehydrogenases (ACDs)[1] are a class of flavoenzymes that catalyze the two-electron oxidation of saturated acyl-CoA thioesters, from 4 to >18 carbons in length. Medium-chain acyl-CoA dehydrogenase (MCAD), having optimal activity for C_8 substrates, is the most thoroughly characterized ACD (*1*). The reaction catalyzed by this enzyme occurs formally in two steps (*2*):

$$\text{E-FAD}_{ox} + \text{SH}_2 \rightleftharpoons \text{E-FADH}_{2red}\text{-P} \quad (1)$$

$$\text{E-FADH}_{2red}\text{-P} + 2\text{ETF}_{ox} \rightleftharpoons \text{E-FAD}_{ox}\text{-P} + 2\text{ETF}_{1e}\text{-} \quad (2)$$

where E is MCAD, FAD is flavin adenine dinucleotide, SH_2 is substrate, P is product, and ETF is electron-transferring flavoprotein. The reductive half-reaction, illustrated in eq 1, involves abstraction of the *pro-R* α-proton from substrate by Glu376 with concerted *pro-R* β-hydride transfer to N(5) of the FAD (*3*−*5*). This results in the formation of a charge transfer (CT) complex between two-electron-reduced MCAD and the *trans*-2-enoyl-CoA thioester. The enzyme is then reoxidized by 2 equiv of ETF (eq 2) in two single-electron transfer steps (*6*, *7*).

Much of the current ACD research focuses on changes in the thermodynamic properties of substrate and enzyme

† This work was supported by a grant from the National Institutes of Health (GM29344) to M.T.S. and by grants from the National Science Foundation (MCB9604254) and the U.S. Army Research Office (DAAG559710083) to P.J.T.

* To whom correspondence should be addressed: phone (612) 624-1019; fax (612) 626-7541; e-mail stankovi@chem.umn.edu.

‡ University of Minnesota.

§ State University of New York.

[1] Abbreviations: CoA, coenzyme A; FAD, flavin adenine dinucleotide; HD-CoA, 2,4-hexadienoyl-coenzyme A; ACD, acyl-coenzyme A dehydrogenase; MCAD, medium-chain acyl-coenzyme A dehydrogenase; ETF, electron-transferring flavoprotein; E-FAD_{ox}, oxidized medium-chain acyl-coenzyme A dehydrogenase; E-$FADH^-_{red}$, two-electron-reduced medium-chain acyl-coenzyme A dehydrogenase; SH_2, substrate (electron and proton donor); P, product (oxidized form of substrate); E_m, midpoint potential; SHE, standard hydrogen electrode; K_{ox}, ionization constant for oxidized medium-chain acyl-coenzyme A dehydrogenase; K_{red}, ionization constant for reduced medium-chain acyl-coenzyme A dehydrogenase; K_{dox}, dissociation constant for oxidized medium-chain acyl-coenzyme A dehydrogenase-bound ligand; K_{dred}, dissociation constant for reduced medium-chain acyl-coenzyme A dehydrogenase-bound ligand; CHES, 2-(*N*-cyclohexylamino)ethanesulfonic acid.

10.1021/bi0006464 CCC: $19.00
Published on Web 10/21/2000

brought about by formation of the ACD·acyl-CoA complex (*8*−*14*). When the thermodynamic properties of substrate and enzyme are examined individually, it appears that both electron and proton transfers from substrates to ACDs are quite energetically unfavorable. For example, the midpoint potential (E_m) for FAD in uncomplexed porcine MCAD (E_m = −145 mV vs SHE, pH 7.6, 25 °C) (*8*) is 107 mV more negative than E_m for the octanoyl-CoA/2-octenoyl-CoA couple (−38 mV; *15*), corresponding to an energy barrier for electron transfer of at least 4.9 kcal mol^{-1}. Likewise, the substrate α-proton is only weakly acidic (p$K_a \approx 21$; *9*) while Glu376, the proposed α-proton abstractor (*5*, *16*, *17*), is not a particularly strong base (p$K_a \approx 6-6.5$; *10*, *12*). Overcoming this 20 kcal mol^{-1} energy barrier, as well as the one imposed by redox potential difference, requires significant thermodynamic modulation of the enzyme and/or substrate.

From previous spectroelectrochemical studies, it has been found that substrate/product binding induces a 120 mV positive shift in the E_m of pig kidney MCAD (*15*). Similar shifts have also been observed in the *Megasphaera elsdenii* short-chain acyl-CoA dehydrogenase (*18*). Until the 2.4 Å crystal structure of MCAD was solved, the possible cause(s) of the potential shifts was unclear (*17*).

In the enzyme·substrate complex, the substrate thioester carbonyl is within hydrogen-bonding distance of the 2′-OH of the ribityl chain of the flavin and the amide N−H of Glu376 (*17*). It is proposed that this hydrogen-bonding network polarizes substrate/product to create partial positive charge near the flavin ring (*19*−*21*) and, as a result, raises the E_m of the enzyme. H-bonding to the carbonyl oxygen is also thought to lower the pK_a of the substrate α-proton by 9−13 pK units (11). Desolvation of the enzyme active site by substrate binding may provide an additional means of thermodynamic regulation. Previous work has shown that the pK_a of Glu376 in oxidized MCAD can be raised at least 3 pK units by the binding of several different product analogues (10, 11, 14).

Much of the previous evidence for substrate/product polarization in ACDs has come from resonance Raman (RR) and NMR studies of reduced MCAD·2-octenoyl-CoA and oxidized MCAD·3-thiaacyl-CoA complexes (*13*, *21*, *22*). In these RR studies, CT bands formed between the analogues and flavin were excited to generate resonance-enhanced Raman signals. Although the studies have provided some of the most critical evidence for substrate polarization to date, the RR approach is limited to complexes that form long-wavelength CT bands. Oxidized MCAD does not form a CT band with 2-enoyl-CoA product analogues, and consequently, these complexes cannot be studied by RR spectroscopy.

Off-resonance Raman studies of ACDs are now possible because of the development of a sensitive Raman system that utilizes red laser excitation, thereby avoiding problems associated with sample fluorescence (*23*, *24*). This system has been used in the past to investigate specific π-electron reorganization occurring in several other coenzyme A-dependent enzymes, including enoyl-CoA hydratase and 4-chlorobenzoate-CoA dehalogenase (*23*, *25*). In the current study, Raman difference spectroscopy is used to characterize the electronic structure of a product analogue, 2,4-hexadienoyl-CoA (HD-CoA; compound **3**, Chart 1), bound to MCAD. The extended π-electron conjugation in the ligand

Chart 1: Acyl-CoA and Enoyl-CoA Analogues Described in This Work

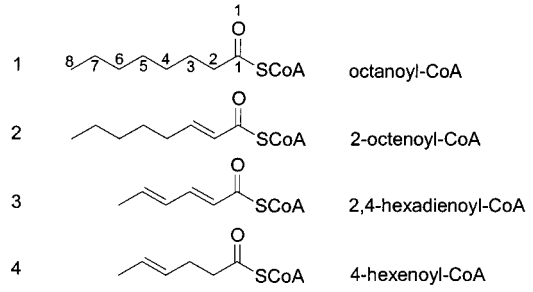

stabilizes the oxidized form of HD-CoA, allowing it to be studied in association with both oxidized and reduced MCAD. The work presented here provides the first direct evidence for *selective* polarization of a product analogue in the active site of oxidized and reduced pig kidney MCAD.

MATERIALS AND METHODS

Materials. Medium-chain acyl-CoA dehydrogenase was purified from pig kidney as described previously (*1*), with the addition of an octyl-Sepharose column to aid in the removal of contaminating enoyl-hydratase activity (*26*). Pig kidneys were purchased from Lindenfelsers Meats (Albertville, MN) and stored at −80 °C prior to enzyme purification. A detailed account of the materials and methods used for MCAD purification in the Stankovich laboratory has been published (*27*).

Preliminary experiments were performed with 2,4-hexadienoyl-CoA (HD-CoA) that was the generous gift of Dr. Vernon Anderson (Case Western Reserve University, Cleveland, OH). For subsequent experiments, HD-CoA and isotopically labeled HD-CoA were synthesized and characterized by the methods described by Tonge et al. (*23*, *28*). Hexadienoic acid, 1,1′-carbonyldiimidazole, acetaldehyde, [1-^{13}C]acetyl chloride, and coenzyme A (lithium salt) were purchased from Sigma Chemical Co. [1,3-$^{13}C_2$]Malonic acid (99% ^{13}C), [2-^{13}C]malonic acid (99% ^{13}C), and $H_2{}^{18}O$ (95−98% ^{18}O) were purchased from Cambridge Isotope Labs. All HD-CoA ligands were lyophilized and stored at −20 °C.

Electrochemical experiments were performed at 25 °C in potassium phosphate and CHES (Sigma) buffer prepared with glass-distilled water. The following dyes were used: methyl viologen (Sigma), indigodisulfonate (Aldrich), and pyocyanine [photochemically synthesized (*29*) from phenazine methosulfate (Sigma)]. Sodium dithionite was purchased from Fisher Scientific.

Equipment. UV−visible spectrophotometric measurements were made on a Perkin-Elmer Lambda 12 spectrophotometer, and Perkin-Elmer Computerized Spectroscopy Software (PECSS), version 4.31, was used for spectral acquisition and manipulation. The spectrophotometer contained a thermostated cell compartment and stirring mechanism. An argon gas line that included an online oxygen scavenger, Riddox (Fisher Scientific), and a connected vacuum system was used for degassing all samples. A Bioanalytical Systems (BAS) BAS-100 or a BAS 50CV electrochemical analyzer was used for coulometric and potentiometric titrations.

The Raman spectra presented here were acquired on an instrument described recently (*14*, *23*, *24*) in which the components have been optimized for operation in the near-

IR to reduce problems associated with large fluorescence backgrounds that can interfere with Raman studies of biological systems. Near-IR excitation (752 nm) was provided by a Model 890 Ti:sapphire laser operated at 700 mW (Coherent, Santa Clara, CA) and pumped by an Innova 308C argon ion laser (Coherent).

General Methods. MCAD used for all experiments was >95% pure as determined by sodium dodecyl sulfate (SDS)−polyacrylamide gel electrophoresis. The activity of MCAD was routinely assayed by use of the DCIP/PMS system described by Thorpe and co-workers (*1*). Concentrations of uncomplexed oxidized MCAD were determined spectrophotometrically with an extinction coefficient of 15.4 mM^{-1} cm^{-1} at 446 nm (*1*). Isotopically labeled and unlabeled HD-CoA analogues were quantified with an extinction coefficient of 19.5 mM^{-1} cm^{-1} at 260 nm (*30*). The binding constant for HD-CoA to oxidized MCAD was determined by spectrophotometric titration of MCAD with HD-CoA (*31*). The change in absorption at 490 nm was followed as a function of the concentration of HD-CoA. Nonlinear regression analysis of the titration was performed using GraphPad Prizm version 3.00 for Windows, GraphPad Software, San Diego, CA (www.graphpad.com).

Electrochemical Methods. Coulometric and potentiometric redox experiments were performed in a spectroelectrochemical cell as described previously (*32*−*34*) at 25 °C unless otherwise indicated. For coulometric reductive titrations, a concentration of 10−20 μM protein in 50 mM potassium phosphate buffer at pH 7.6 was used with 0.1 mM methyl viologen added to mediate MCAD reduction.

Potentiometric titrations were performed under similar conditions as coulometric titrations, but in addition to methyl viologen, indigo disulfonate ($E_m = -0.118$ V at pH 7.6; *35*) and pyocyanine ($E_m = -0.019$ V at pH 7.6; *35*) were added (2−5 μM) to facilitate equilibration between the protein and working electrode. Equilibration typically took 1−2 h and was defined by a change in potential of <1 mV/10 min. All potential values reported herein are versus the standard hydrogen electrode (SHE).

Experiments at pH 6.5−8.2 were performed in 50 mM potassium phosphate buffer. A 50 mM potassium phosphate/20 mM CHES buffer was used for titrations at pH 8.5, 9.0, and 10.0. The ionic strengths for all buffering systems in the pH study were maintained at 100 mM as redox potentials have been shown to be ionic strength-dependent (*36*).

Calculations for Coulometric and Potentiometric Titrations. If necessary, spectra were corrected for turbidity before quantitation (*37*). For coulometric titrations, the number of reducing equivalents, *n*, was calculated on the basis of the moles of enzyme in the sample:

$$n = \frac{Q}{NF} \tag{3}$$

where Q is the amount of charge added to the system in coulombs, N is the number of moles of species in solution, and F is Faraday's constant (96 485 C mol^{-1}). Since complete reduction of oxidized FAD to hydroquinone requires two electrons, an $n = 2$ for flavin reduction is expected.

By use of spectral data and the measured potential at each point during the titration, the Nernst equation can be applied to determine the midpoint potential of the enzyme:

$$E = E_m + 2.303\frac{RT}{nF}\log\frac{[\text{oxidized}]}{[\text{reduced}]} \tag{4}$$

where E is the measured equilibrium potential at each point in the titration, R is the gas constant (8.31441 J mol^{-1} K^{-1}), T is the experimental temperature in kelvins, and F is Faraday's constant as defined previously. A Nernst plot (E vs log [oxidized]/[reduced]) is constructed and E_m, the midpoint potential of the half-reaction, is given by the y-intercept. The number of electrons transferred, n, can be calculated from the slope of the Nernst plot. Typical error for experimentally determined midpoint potentials is ±2−5 mV (*8*).

Midpoint potentials were acquired over a wide pH range and pK_a values were determined by fitting the data to a redox-linked ionization model described by Clark (*35*):

$$E_m = E_0 - 0.0592\text{pH} + 2.303\frac{RT}{nF}\log\left(\frac{[H^+]^3 + [H^+]^2K_{red,1} + [H^+]K_{red,1}K_{red,2} + K_{red,1}K_{red,2}K_{red,3}}{[H^+]^3 + [H^+]^2K_{ox,1} + [H^+]K_{ox,1}K_{ox,2} + K_{ox,1}K_{ox,2}K_{ox,3}}\right) \tag{5}$$

where E_0 is a calculated constant corresponding to E_m at pH 0 and $[H^+]$ is the hydrogen ion concentration. The various Ks are assigned in the text as pK_as.

Dissociation constants for the reduced MCAD·HD-CoA complex, K_{dred}, were calculated from the dissociation constant of the oxidized enzyme complex, K_{dox}, and the midpoint potentials for both the free and bound MCAD. To determine K_{dred} the following equation was used:

$$K_{dred} = K_{dox} \times 10^{-[([E_{m(bound)} - E_{m(free)}]nF)/(2.303RT)]} \tag{6}$$

However, under some of the conditions used in this work, the enzyme was not fully saturated with HD-CoA. Equation 7 was derived to calculate dissociation constants for the reduced enzyme·HD-CoA complex under nonsaturating conditions and when the concentration of HD-CoA is on the same order of magnitude as the enzyme concentration. From eqs 7−9, K_{dred} can be solved at any experimental ligand concentration (L_T). If a ligand concentration that fulfills enzyme saturation conditions is substituted into eq 7, the midpoint potential for the enzyme·ligand complex is obtained.

$$E_m[L] = E_m(\text{free}) + 2.303\frac{RT}{nF}\log\left(\frac{1 + \dfrac{L_T - [EL]_{red}}{K_{red}}}{1 + \dfrac{L_T - [EL]_{ox}}{K_{dox}}}\right) \tag{7}$$

where

$$[EL]_{ox} = \frac{(K_{dox} + L_T + E_T) - \sqrt{(K_{dox} + L_T + E_T)^2 - 4L_TE_T}}{2} \tag{8}$$

and

$$[EL]_{red} = \frac{(K_{dred} + L_T + E_T) - \sqrt{(K_{dred} + L_T + E_T)^2 - 4L_T E_T}}{2} \quad (9)$$

Under conditions where L_T is significantly greater than E_T, eq 7 collapses to

$$E_m[L] = E_m(\text{free}) + 2.303\frac{RT}{nF}\log\left(\frac{1 + \frac{L_T}{K_{red}}}{1 + \frac{L_T}{K_{ox}}}\right) \quad (10)$$

The variables in eqs 7−10 that have yet to be defined are $E_m[L]$, the enzyme midpoint potential in the presence of a defined concentration of ligand; E_T, the total concentration of enzyme in all oxidation and binding states; L_T, the total concentration of ligand in all binding states; $[EL]_{ox}$, the concentration of oxidized enzyme complexed with ligand; and $[EL]_{red}$, the concentration of reduced enzyme complexed with ligand.

Raman Spectroscopy. Raman measurements of oxidized MCAD were made by adding 60 μL of enzyme (200−400 μM) to a 2 mm by 2 mm rectangular quartz cell. Spectra were then collected for 8 min before addition of HD-CoA (typically 1 or 2 μL of about 10 mM product analogue) to the same cell; care was taken not to perturb the optical alignment or cell position. The reduced enzyme spectra were generated by adding approximately 1 molar equiv of degassed dithionite solution to the enzyme before addition of HD-CoA. All the reduced spectra were acquired from a specially designed anaerobic Raman cell. Raman difference spectra were calculated by performing a computer subtraction of the spectrum of the enzyme in buffer alone from the spectra of MCAD in the presence of HD-CoA. An appropriate scaling factor was applied to remove any residual protein signals. The difference spectra presented here are wavenumber-calibrated against cyclohexanone and are accurate to ±2 cm^{-1}. All spectral manipulations were carried out with WinIR software and data acquisition was with WinSpec (Princeton Instruments). The resolution of the Raman system is approximately 10 cm^{-1} under the conditions used for acquiring the reported spectra.

RESULTS

Formation of Medium-Chain Acyl-CoA·Hexadienoyl-CoA Complex. Figure 1 (—) shows the spectrum of free MCAD, which has an extinction coefficient at 446 nm of 15.4 mM^{-1} cm^{-1} (*1*). This flavin band was red-shifted and the intensity was slightly quenched to an extinction coefficient of 15.1 mM^{-1} cm^{-1} at 456 nm (Figure 1, ---) when the enzyme was 96% saturated with HD-CoA. This behavior is typical for the binding of analogues to oxidized ACDs and is attributed to desolvation of the enzyme active site (*5*, *9*, *38*−*40*). No long-wavelength CT band was observed after incubation of oxidized MCAD with HD-CoA for 24 h at 4 °C (data not shown), indicating that the enzyme does not have hydratase activity toward HD-CoA. The binding constant for HD-CoA to oxidized MCAD was determined by spectrophotometric

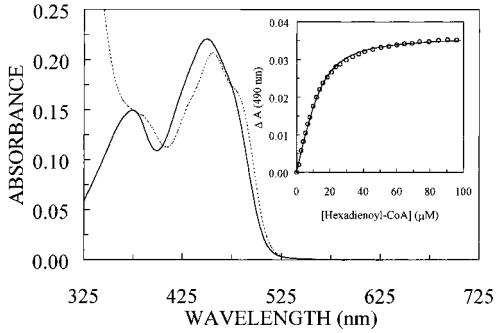

FIGURE 1: Spectra of MCAD (14.3 μM) in the absence (—) and presence (---) of HD-CoA (96 μM). Spectra were recorded at 25 °C in 50 mM potassium phosphate buffer, pH 7.6. Inset: Plot of change in absorbance at 490 nm upon titration of MCAD with HD-CoA (○). Fit to K_{dox} of 3.5 ± 0.1 μM (—).

titration of MCAD (14.3 μM) with 1 mM HD-CoA. The change in absorption at 490 nm was followed as a function of the concentration of HD-CoA (inset, Figure 1), and a K_{dox} of 3.5 ± 0.1 μM was obtained from a nonlinear regression fit of the data.

Coulometric Titrations of Hexadienoyl-CoA-Complexed MCAD. Coulometric reductions were performed to determine if the oxidation state of HD-CoA remains unperturbed throughout the majority of the reduction of the enzyme. The stabilization of a single ligand form to both oxidized and reduced enzyme is ideal for interpretation of potentiometric titration and Raman data. The coulometric titration shown in Figure 2A was performed at a HD-CoA concentration such that 95% of the oxidized enzyme was in complex with the analogue. The titration appears to consist of two reductive events. The absorbance at 456 nm decreased sharply ($\Delta A = -0.20$) during the first part of the titration due to reduction of the flavin. An increase in absorbance at 570 nm ($\Delta A = 0.030$) accompanied flavin reduction, consistent with formation of a CT complex between the dienoyl ligand and reduced MCAD. The absorbance at 570 nm reached a maximum between 2.6 and 3.0 reducing equivalents, with the majority of the 456 nm absorbance decrease occurring during this part of the titration as well. From $n \approx 3.0$ to $n \approx 11.8$ the absorbance due to the CT band decreased somewhat linearly ($\Delta A = -0.025$), consistent with the formation of a complex between reduced MCAD and a ligand saturated at the C(2)−C(3) position. After 11.8 reducing equivalents had been added, reduced methyl viologen was thermodynamically stabilized, indicating that all species with redox potentials more positive than −449 mV had been reduced (*35*).

Since more than 2 reducing equivalents could be added to the system, it became apparent that both the flavin and HD-CoA were undergoing reduction. To determine if one or both double bonds of HD-CoA were reduced, coulometric reduction of MCAD was performed at several different HD-CoA concentrations. A plot of *n* total versus the number of moles of HD-CoA per mole of enzyme is shown in Figure 2B (○) and clearly indicates that the reduction of the HD-CoA is a two-electron process (one double bond is reduced), with an additional two electrons required to completely reduce the enzyme-bound FAD. The decay of the charge-transfer band in Figure 2A suggests that the two-electron reduced product remains unsaturated at the C(4)═C(5) position (compound **4**, Chart 1) rather than the C(2)═C(3)

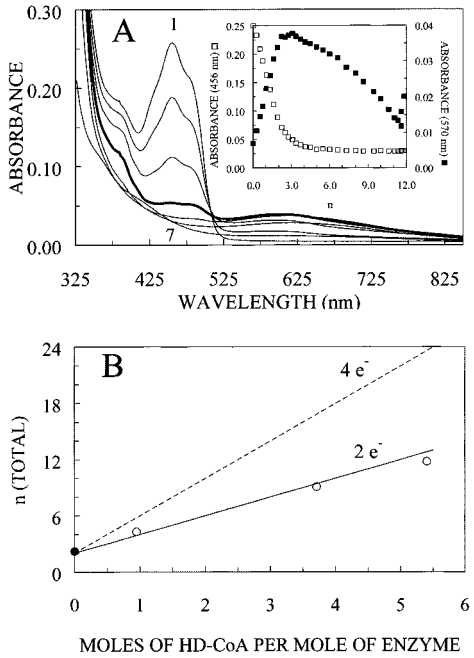

FIGURE 2: Coulometric reductions of MCAD·HD-CoA complexes. Titrations were performed under anaerobic conditions at 25 °C in 50 mM potassium phosphate buffer, pH 7.6. (A) Coulometric reduction of MCAD (14.7 μM) in the presence of HD-CoA (80 μM) and methyl viologen (100 μM). Only selected spectra are shown for clarity. Curves 1−7: n = 0.0, 1.0, 1.8, 2.6 (bold), 4.7, 8.2, and 11.8, respectively. Inset: Plot of absorbance at 456 nm (□) and 570 nm (■) as a function of the number of reducing equivalents (n) added during the titration. (B) Correlation between the total number of reducing equivalents (n) and the amount of HD-CoA in solution. Datum at 0 μM HD-CoA (●) was obtained from ref *37*. All other data (○) were obtained from coulometric titrations in this work. Concentrations of HD-CoA were varied from 14.3 to 80 μM. Enzyme concentrations were kept between 13.8 and 14.8 μM. Theoretical fits are shown for two- (—) and four- (---) electron reduction of HD-CoA.

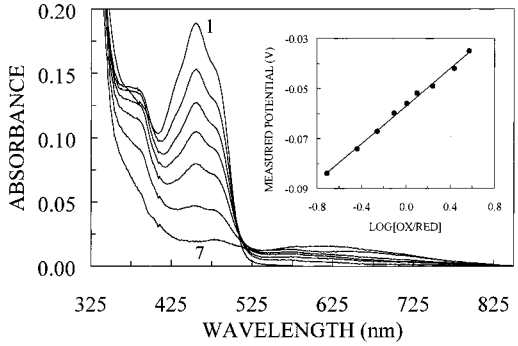

FIGURE 3: Potentiometric titration of MCAD (10.7 μM) in the presence of HD-CoA (181 μM). Methyl viologen (100 μM) serves as a redox mediator. Redox indicators are pyocyanine (5.0 μM) and indigo disulfonate (2.5 μM). Titration was performed under anaerobic conditions at 25 °C in 50 mM potassium phosphate buffer, pH 7.6. Intermediate spectra have been removed for clarity. The spectrum of the oxidized MCAD·HD-CoA complex is shown by curve 1. Curves 2−6 show the complex at E = −30, −44, −51, −62, and −79 mV vs SHE. Curve 7 is the spectrum of the fully reduced MCAD bound to HD-CoA. Inset: Nernst plot indicating an E_m = −0.052 V and an n = 1.6.

Table 1: Midpoint Potentials of Free MCAD and HD-CoA-Bound MCAD at Indicated pH Values

	E_m (V)			
pH	MCAD[a] free	HD-CoA·MCAD (uncorrected)	HD-CoA·MCAD (corrected)	ΔE_m[b] (V)
6.5	−0.083	−0.011	−0.009	+0.074
7.1	−0.114	−0.047	−0.043	+0.071
7.6	−0.145	−0.054	−0.052	+0.093
8.0	−0.168	−0.073	−0.070	+0.098
8.2	−0.180	−0.083	−0.079	+0.101
8.5	−0.189	−0.098	−0.094	+0.095
9.0	−0.210	−0.141	−0.138	+0.072
10.0	−0.263	−0.178	−0.175	+0.088

[a] From ref 8. [b] Comparison of free MCAD and corrected HD-CoA-bound MCAD.

position. A CT-complex between reduced MCAD and 2-hexenoyl-CoA would be expected if only the C(4)═C(5) bond was reduced.

Two important conclusions can be drawn from the coulometric titrations. First, these titrations show that HD-CoA remains oxidized throughout the enzyme reduction and should therefore serve as an excellent analogue for other electrochemical and Raman studies with both oxidized and reduced MCAD. Reduction of the product analogue occurs only after MCAD has been reduced. The second notable finding is that HD-CoA reduction is limited to the C(2)═C(3) portion of the chain. The C(4)═C(5) bond is stable in the presence of MCAD to at least −449 mV.

pH Dependence of the Redox Potential of Hexadienoyl-CoA-Complexed MCAD. Midpoint potentials for MCAD·HD-CoA complexes were determined at several pHs. A representative potentiometric titration at pH 7.6 is shown in Figure 3. As a result of the formation of the long-wavelength CT band, it is difficult to accurately quantitate the amount of semiquinone that may have been stabilized during the titration. Consequently, the midpoint potentials reported are for the oxidized FAD/hydroquinone couple. The E_m of −52 mV (inset, Figure 3) for the MCAD·HD-CoA complex is 93 mV more positive than the midpoint potential of free MCAD (E_m = −145 mV; *20*), indicating a significant potential shift in the enzyme upon binding HD-CoA. Equation 6 can be used to calculate a dissociation constant for the analogue and reduced enzyme (K_{dred}) of 2.5 nM, a 1400-fold difference between K_{dox} (3.5 μM) and K_{dred}. Tighter binding of product or a 2-enoyl-CoA product analogue to reduced enzyme is consistent with previous work on ACDs (*20, 31*).

Potentiometric titrations of MCAD in the presence of HD-CoA were performed at pHs between 6.5 and 10.0 to calculate pK_as of key amino acid residues in the enzyme active site. Precipitation of the enzyme at pHs below 6.0 and enzyme denaturation above pH 10.0 precluded studies under more acidic and basic conditions (*41*). Table 1 shows the E_ms determined at each pH for free MCAD and the MCAD·HD-CoA complex. It should be noted that many of the midpoint potentials were not determined at saturating HD-CoA concentrations. In most cases, only 80−90% of the enzyme was in the complexed form. To calculate E_m under saturating conditions, eq 7 was applied in the manner described under Calculations for Coulometric and Potentiometric Titrations. Both saturation-corrected and uncorrected potentials are given in Table 1. In the titration presented in Figure 3, the potential of MCAD was determined under near-saturating conditions (98%) and validates the use of eq 7. The measured potential of −52 mV is identical to the corrected value obtained from an average of four experiments run under subsaturating conditions at pH 7.6.

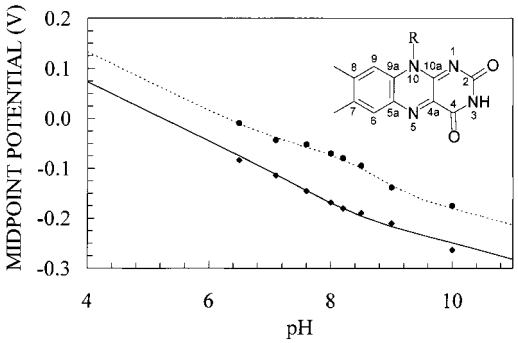

FIGURE 4: pH vs midpoint potential for uncomplexed MCAD (◆) and HD-CoA-bound MCAD (●). Midpoint potential values are from Table 1. Fits for uncomplexed MCAD (—) and HD-CoA bound MCAD (---) were obtained from eq 5. Inset: Numbering scheme for isoalloxazine ring of FAD.

Corrected midpoint potentials at each pH were then fit to the redox-linked ionization model described by eq 5. Assignment of pK_as for HD-CoA-complexed MCAD was done with the pK_as previously determined for uncomplexed enzyme as a first approximation (*12*). Refinement of the pK_a values to fit the data in Figure 4 (●) yielded the pK_as shown in Table 2. As with the uncomplexed pig kidney MCAD (*12*), p$K_{ox,3}$ and p$K_{red,1}$ were assigned to N(3) and N(1) of the flavin, p$K_{ox,1}$ and p$K_{red,2}$ were assigned to Glu376, and p$K_{ox,2}$ and p$K_{red,3}$ were assigned to Glu99.

From the slopes of the fits, the number of protons transferred over various pH ranges can be estimated. For the HD-CoA-bound MCAD (---, Figure 4), the overall slope of 47 mV/pH unit from pH 6.5 to 10.0 is between what is expected for a $2e^-/1H^+$ (30 mV/pH) and a $2e^-/2H^+$ (59 mV/pH) transfer. Uncomplexed pig kidney MCAD (—, Figure 4) showed definite $2e^-/2H^+$ transfer behavior over this same pH region (*12*). More detailed analysis of the HD-CoA-complexed MCAD data reveals that the slope from about pH 7.0 to 8.0 is consistent with $2e^-/1H^+$ transfer, whereas the slope from pH 8.0 to around pH 9.5 shows $2e^-/2H^+$ transfer characteristics.

For free MCAD, slight changes in the slope near pH 7.0 and 8.0 have been noted (*12*). Indeed, several pK_as are assigned for the enzyme and flavin in this region (Table 2). For the HD-CoA·MCAD complex, a slope change occurs around pH 9.5 in addition to changes at pH 7.0 and pH 8.0. The pK_as for Glu376 in both the oxidized (9.3) and reduced (9.8) enzyme assigned in this region are significantly larger than the pK_as calculated for the base in the free oxidized (6.5) and reduced (7.9) enzyme (*12*). These pK_a shifts indicate that, upon analogue binding, Glu376 becomes a stronger base, regardless of the enzyme oxidation state.

At pH 7.1, the reductive half-reaction can be written as

$$\text{E-FAD}_{ox} + 2e^- + 1H^+ \rightleftharpoons \text{E-FADH}_{red\text{-}} \qquad E_m = -0.043\ \text{V} \quad (11)$$

where the lone proton is transferred to the N(5) position of reduced FAD. At this pH, Glu99 and Glu376 should be protonated in both oxidized and reduced MCAD. However, at pH 8.2, the reduction occurs as

$$\text{E-FAD}_{ox} + 2e^- + 2H^+ \rightleftharpoons \text{EH}^+\text{-FADH}_{red\text{-}} \qquad E_m = -0.079\ \text{V} \quad (12)$$

Table 2: pK Values Assigned to Fit E_m Data Shown in Figure 4 for Oxidized (pK_{ox}) and Reduced (pK_{red}) Enzyme

pK	assignment	MCAD[a]	HD-CoA·MCAD
p$K_{ox,1}$	Glu376 (ox)	6.5	9.3
p$K_{ox,2}$	Glu99 (ox)	7.5	7.4
p$K_{ox,3}$	N(3) flavin	11.5	11.5
p$K_{red,1}$	N(1) flavin	6.5	6.9
p$K_{red,2}$	Glu376 (red)	7.9	9.8
p$K_{red,3}$	Glu99 (red)	8.5	8.6

[a] From ref *12*.

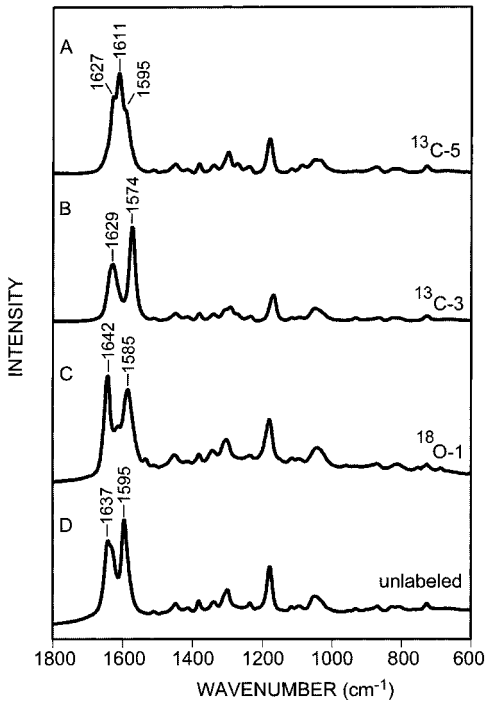

FIGURE 5: Raman spectra of HD-CoA in 50 mM potassium phosphate buffer, pH 7.6. (A) ^{13}C(5)-Labeled HD-CoA (8.6 mM); (B) ^{13}C(3)-labeled HD-CoA (14.8 mM); (C) ^{18}O(1)-labeled HD-CoA (16.3 mM); (D) unlabeled HD-CoA (12.4 mM).

where the second proton is taken up by Glu99 upon enzyme reduction.

Raman Difference Spectra of Hexadienoyl-CoA Bound to Oxidized MCAD. Figure 5 shows the Raman difference spectra of HD-CoA and three isotopically labeled analogues [^{18}O(1), ^{13}C(3), and ^{13}C(5)] in aqueous solution. On the basis of earlier isotopically labeled HD-CoA studies (*23*, *28*), the two most prominent Raman bands in unlabeled HD-CoA, near 1595 and 1637 cm^{-1}, have been assigned to normal modes involving C═C stretching in the hexadienoyl region. These C═C stretching modes are further influenced by vibrational coupling with the thioester carbonyl group.

The Raman difference spectra of HD-CoA and the isotopically labeled analogues bound to oxidized MCAD are presented in Figure 6. The Raman spectra below 1500 cm^{-1} are composed of vibrational modes due to HD-CoA as well as positive/negative features arising from flavin vibrational modes that are perturbed on binding HD-CoA to MCAD. Further analysis of this region of the spectrum will provide important information on the modulation in flavin structure that occurs upon formation of the MCAD·HD-CoA complex. In the present study, the focus is on the polarization of the product analogue by the enzyme active site as revealed by

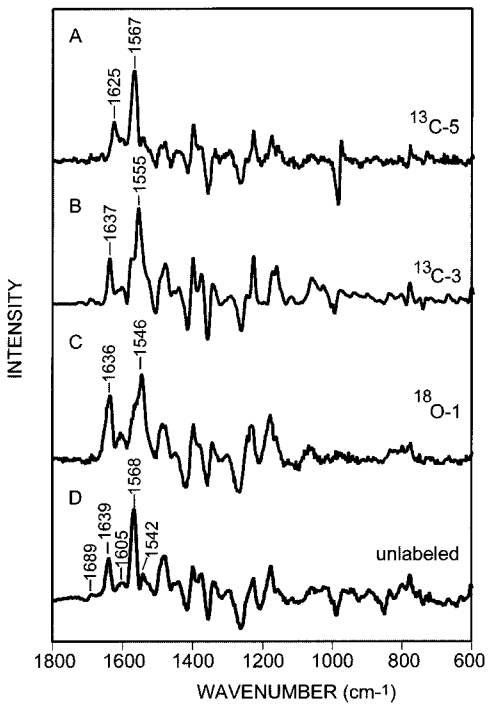

FIGURE 6: Raman difference spectra of oxidized MCAD complexed with HD-CoA (0.8 equiv) in 50 mM potassium phosphate buffer, pH 7.6. (A) MCAD (400 μM) complexed with ^{13}C(5)-labeled HD-CoA; (B) MCAD (400 μM) complexed with ^{13}C(3)-labeled HD-CoA; (C) MCAD (380 μM) complexed with ^{18}O(1)-labeled HD-CoA; (D) MCAD (380 μM) complexed with unlabeled HD-CoA.

changes that occur on binding in the double-bond stretching region (1500−1800 cm^{-1}). Two prominent bands are observed at 1639 and 1568 cm^{-1} in the unlabeled bound HD-CoA spectrum (Figure 6). The band at 1568 cm^{-1} is sensitive to both ^{18}O(1) and ^{13}C(3) labeling but not to ^{13}C(5) labeling, identifying its assignment to the C(3)═C(2)−C(1)═O enone fragment of HD-CoA. The second prominent band at 1639 cm^{-1} is not sensitive to either ^{13}C(3) or ^{18}O(1) labeling but does shift to 1625 cm^{-1} on ^{13}C(5) labeling (Figure 6). Thus, this band is assigned to a normal mode localized on the terminal C(4)═C(5) bond.

The other bands observed in this region at 1689, 1605, and 1542 cm^{-1} are not sensitive to labeling of HD-CoA and are most likely associated with the flavin. A large body of literature exists on the vibrational modes of flavins and flavoproteins (*42*). The band at 1689 cm^{-1} can be assigned predominantly to the C(4)═O mode of the bound flavin (*43*, *44*). Detailed studies on a series of enzymes, including acyl-CoA dehydrogenases, containing isotopically labeled flavins have revealed that the position of this band, which appears around 1710 cm^{-1} in free flavin, is dependent on the strength of hydrogen bonding to the C(4)═O group (*44*). Similarly, these studies assigned a band in the range 1602−1620 cm^{-1} predominantly to a C(4a)═C(10a) stretching mode. In our data this band appears at 1605 cm^{-1} (Table 3). The third flavin band in this region at 1542 cm^{-1} can probably be assigned to a mode involving N(5)−C(4a), N(1)−C(10a), and C(4a)−C(10a), which is sensitive to hydrogen bonding at N(1) and N(5) (*45*). More accurate assignments will be forthcoming from detailed isotope labeling studies of the flavin.

Raman Difference Spectra of HD-CoA Bound to Reduced MCAD. The Raman difference spectra of HD-CoA and the isotopically labeled analogues bound to reduced MCAD are presented in Figure 7. The formation of a charge-transfer complex between HD-CoA and the reduced form of the enzyme results in some dramatic changes in the Raman spectra relative to those of the oxidized form. These changes are due to preresonance enhancement of those normal modes that involve contributions from the specific vibrational coordinates of both the flavin and HD-CoA structures participating in the charge-transfer complex. This results in

Table 3: Raman Band Positions in the Double-Bond Stretching Region for HD-CoA and Three Isotopically Labeled Analogues [^{18}O(1), ^{13}C(3), and ^{13}C(5)] Free and Bound to Oxidized and Reduced MCAD

enzyme	isotope	HD bands (cm^{-1})		flavin bands (cm^{-1})	
none[a]	unlabeled	1637	1595	none	none
	^{18}O(1)	1642	1585	none	none
	^{13}C(3)	1629	1574	none	none
	^{13}C(5)	1627	1595	none	none
MCAD (oxidized)	unlabeled	1639	1568	1605	1542
	^{18}O(1)	1636	1546 (1567 sh)	1606	buried
	^{13}C(3)	1637	1555 (1570 sh)	1602	buried
	^{13}C(5)	1625	1567	1603	1543
MCAD (reduced)	unlabeled	1641 (w)	1567 (vs)	1609 (vs)	1531 (vs)
	^{18}O(1)	1639 (w)	1553 (vs)	1608 (vs)	1526 (vs)
	^{13}C(3)	1638 (w)	1558 (vs)	1610 (vs)	1531 (vs)
	^{13}C(5)	buried	1568 (vs)	1612 (vs)	1530 (vs)

[a] From refs 23 and 28. Band positions are given in wavenumbers; (sh) shoulder, (w) weak band, (vs) very strong band.

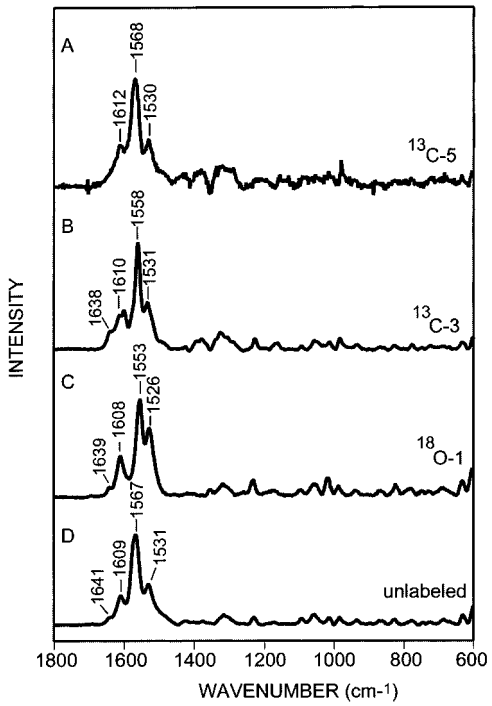

FIGURE 7: Raman difference spectra of reduced MCAD complexed with HD-CoA (0.8 equiv) in 50 mM potassium phosphate buffer, pH 7.6. (A) MCAD (150 μM) complexed with ^{13}C(5)-labeled HD-CoA; (B) MCAD (200 μM) complexed with ^{13}C(3)-labeled HD-CoA; (C) MCAD (380 μM) complexed with ^{18}O(1)-labeled HD-CoA; (D) MCAD (380 μM) complexed with unlabeled HD-CoA. In each case 1 molar equiv of dithionite was added to reduce the enzyme prior to addition of HD-CoA.

a strong increase in the Raman band intensities of particular normal modes upon complex formation.

For unlabeled HD-CoA bound to reduced MCAD, intense bands are observed at 1609, 1567, and 1531 cm^{-1}. The 1567 cm^{-1} band is sensitive to isotopic substitution, shifting to 1553 and 1558 cm^{-1} upon $^{18}O(1)$ and $^{13}C(3)$ labeling of HD-CoA. However, no shift is observed for $^{13}C(5)$-labeled HD-CoA (Table 3). Consequently, this band is assigned to the hexadienoyl moiety and, on the basis of the similarity in the isotopic shifts, is the counterpart of the band observed at 1568 cm^{-1} in the oxidized spectrum (Figure 6). The isotope data reveal that this particular band arises from a normal mode that involves contributions from the stretching motions of the hexadienoyl C(1)═O group and the C(2)═C(3) double bond. Another HD-CoA band also appears as a shoulder near 1640 cm^{-1}. The weak Raman intensity of this band indicates that the vibrational coordinates contributing to this particular normal mode are not participating in the charge-transfer complex. The sensitivity of the band to $^{13}C(5)$ labeling reveals it to be an HD-CoA mode similar to that observed near 1640 cm^{-1} when bound to oxidized MCAD.

The two other intense bands at 1531 and 1609 cm^{-1} are assigned to flavin modes with contributions from bonds that are involved in the charge-transfer complex. The 1531 cm^{-1} band is also found to be slightly sensitive to labeling, shifting to 1526 cm^{-1} in $^{18}O(1)$-labeled HD-CoA. This would seem to indicate that there is some component from HD-CoA, but this point is unclear since a flavin mode, similar to the band at 1542 cm^{-1} in the oxidized spectrum, is expected to contribute at this position. Thus, we assign this band to the N(5)−C(4a), N(1)−C(10a), and C(4a)−C(10a) stretching coordinates with the possibility of some coupling with the hexadienoyl carbonyl. The 1609 cm^{-1} band is assigned to the same flavin mode as appears in the oxidized form at 1605 cm^{-1}. In contrast to the oxidized form of the enzyme, all the spectral features below 1500 cm^{-1} are positive. This reflects the sharp increase in the Raman intensity of both HD-CoA and flavin modes that occur on formation of the charge-transfer complex.

DISCUSSION

This paper demonstrates the ability of HD-CoA to serve as a product analogue for both electrochemical and Raman studies. As a result, direct evidence for substrate polarization and redox potential shifts has been obtained for the first time to our knowledge for the same analogue. In previous electrochemical studies (*20*, *31*), the effects of ligand binding on the redox potentials of MCAD were examined with analogues altered from natural substrate/product by substitution at either the C(2) or C(3) position, preventing electron transfer between the analogue and enzyme during MCAD reduction. Unlike 3-thia- and 2-azaacyl-CoA thioesters, HD-CoA maintains an electronic structure in the C(3)═C(2)−C(1)═O region that is similar to natural *trans*-2-enoyl-CoA products, allowing the analogue to engage in a CT complex with reduced enzyme (Figure 2A). The only difference between these natural products and HD-CoA is that the latter has a second double bond at the C(4)═C(5) position. This extended conjugation allows HD-CoA to remain oxidized under conditions that cause natural products to reduce.

Binding of HD-CoA to pig kidney MCAD resulted in positive enzyme redox potential shifts at pHs between 6.5 and 10.0 (Table 1). The +93 mV shift at pH 7.6 represents 78% of the shift (+119 mV) reported for MCAD associated with a mixture of octanoyl-CoA/*trans*-2-octenoyl-CoA (*15*). Much of the 26 mV difference may be attributed to chain-length differences between HD-CoA (C_6) and octanoyl-CoA/*trans*-2-octenoyl-CoA (C_8) as C_8 substrates and analogues have been shown to be optimal for MCAD activity (*1*, *9*), inducing pK_a shifts (*10*), as well as stabilization of reduced MCAD (*20*). For example, binding of 2-azaoctanoyl-CoA to MCAD raised the E_m of the enzyme by 74 mV, whereas the four-carbon-shorter 2-azabutyryl-CoA only increased E_m by 33 mV (*20*). Therefore, it is likely that a C_8 analogue such as 2,4-octadienoyl-CoA would induce an enzyme redox potential shift much closer to that observed with octanoyl-CoA/*trans*-2-octenoyl-CoA.

The redox potential of the MCAD·HD-CoA complex exhibits a dependence on pH (Figure 4) consistent with redox-linked ionization of three groups (eq 5). The pK_as determined for these groups (Table 2) indicate that the ionization of two glutamic acids in the active site are influenced by HD-CoA binding as well as the oxidation state of the enzyme-bound flavin. These pK_a changes can most easily be understood by examining the structural and electronic changes that occur in the active site during HD-CoA binding and FAD reduction.

The active site of uncomplexed pig kidney MCAD contains a string of five ordered water molecules held in place by hydrogen bonds formed with the ribityl-2′-OH group of the FAD and the carboxylate oxygens of Glu99 and Glu376 (*17*, *46*). From previous electrochemical work, a $pK_{ox,1} \approx 6.5$ has been assigned for the Glu376 in this enzyme conformation (*12*). It was apparent, however, that a base of this pK would be too weak to abstract the α-proton from an enzyme-complexed acyl-CoA thioester ($pK_a \approx 8-12$; *11*). For efficient catalysis, the pK_a of Glu376 must be raised several units.

Four of the five waters were found to be displaced when octanoyl-CoA/*trans*-2-octenoyl-CoA was soaked into MCAD crystals (*47*). This observation, coupled with additional experimental evidence, suggested that protonated Glu376 is stabilized by ligand-induced active-site desolvation (*10*, *11*, *14*). This notion is supported by our work as the $pK_{ox,1}$ of Glu376 is increased 2.8 units to 9.3 upon HD-CoA binding to oxidized enzyme. An identical pK (apparent) has been reported by Trievel et al. (*9*) for MCAD bound to the product analogue, 4-thiaoctenoyl-CoA. However, in that study it was only possible to follow the relative amounts of the polarized and nonpolarized forms of the ligand bound to *oxidized* enzyme, preventing estimates for ionization constants in *reduced* MCAD complexes. Because the E_m of the enzyme·HD-CoA complex is influenced by the ionization state of Glu376 in both enzyme oxidation states, we are able to assign pK_as in reduced as well as oxidized MCAD. The $pK_{red,2}$ of Glu376 in the reduced enzyme was also found to increase upon HD-CoA binding, from 7.9 to 9.8 (Table 2), indicating that, at physiological pHs, the residue will remain protonated until product is released from the enzyme active site. Although this 1.9 unit pK_a shift is significant, it is 0.9 unit smaller than the shift caused by HD-CoA binding to oxidized enzyme. This discrepancy warrants further discussion and will be addressed below.

Somewhat surprisingly, the pK_a of the second carboxylate in the active site, Glu99, does not change dramatically upon HD-CoA binding to oxidized (7.5 to 7.4) or reduced (8.5 to 8.6) MCAD. Glu99 is located at the bottom of the enzyme active site with the carboxylate bridging the last two of the five water molecules (*17, 46, 47*). It would seem that ligand-induced active-site desolvation should have the same effect on the pK_a of Glu99 as it does on Glu376. Indeed, Vock et al. (*11*) noted a slight increase in the pK_a of Glu99 (from 7.3 to ≈8) when human wild-type MCAD was titrated with the product analogue *p*-NO_2-phenylacetyl-CoA. The lack of a significant Glu99 pK_a shift in the system under current study, however, may be the result of inadequate desolvation of the enzyme active site by HD-CoA. Additional crystallographic studies have shown that only three of the five water molecules are removed by binding hexanoyl-CoA/*trans*-2-hexenoyl-CoA (*46, 47*), suggesting that two waters may remain in close proximity to Glu99 when MCAD binds the C_6-dienoyl molecule. If the protein and solvent environments directly surrounding Glu99 are unaffected by HD-CoA binding, the pK_a of Glu99 should remain unperturbed.

In addition to raising the pK_a of active-site carboxylates, substrate/product binding is proposed to induce polarization in the thioester carbonyl region of the ligands (*20*−*22*). The extent of the π-electron reorganization can be assessed by Raman difference spectroscopy (*23, 25*). The Raman spectra of hexadienoyl-CoA bound to oxidized and reduced MCAD (Figures 6 and 7) show several differences when compared with that of free HD-CoA (Figure 5). Most notably, the stretching mode in the C(3)═C(2)−C(1)═O region shifts from 1595 cm^{-1} in the free form to 1568 and 1567 cm^{-1} in complexes with oxidized and reduced MCAD, respectively (Table 3). This decrease in band frequency is similar to the 1627 to 1577 cm^{-1} shift previously reported for 2-octenonyl-CoA (natural product) binding to reduced MCAD (*21*). Nishina et al. (*21, 22*) suggested that, in this charge-transfer complex, 2-octenoyl-CoA is polarized with appreciable contribution from a resonance structure such as R-$^{+}$C(3)H−C(2)H═C(1)−O^{-}. The present results indicate that formation of the CT complex is not necessary for such polarization. The shift of the 1595 cm^{-1} band is nearly identical for HD-CoA binding to oxidized (no CT band) and reduced MCAD.

Also of interest is the lack of a large shift for the second major HD-CoA band at 1637 cm^{-1}. For HD-CoA in solution (Figure 5) this band is attributed primarily to C═C stretching modes coupled with the carbonyl group as the position of the band is sensitive to $^{18}O(1)$, $^{13}C(3)$, and $^{13}C(5)$ labeling. However, when HD-CoA binds to oxidized MCAD, the band at 1639 cm^{-1} is only sensitive to $^{13}C(5)$ labeling (the band is buried in the spectra for the reduced MCAD complex). This suggests that the active site of MCAD is disrupting π-electron conjugation in the hexadienoyl region of the analogue. The normal mode involving C(4)═C(5) stretching becomes isolated from modes involving stretching in the C(3)═C(2)−C(1)═O enone fragment.

These results indicate not only that HD-CoA is polarized in the active site of MCAD but also that the polarization is limited to the C(3)═C(2)−C(1)═O region. Only minor π-electron rearrangement occurs in the C(4)═C(5) bond due to loss of conjugation. As a result, polarization of hexadienoyl-CoA is likely to occur as shown is Scheme 1, with a partial positive charge developing around carbon 3. A decrease in electron density in this solvent-excluded region, only 3.3 Å from the isoalloxazine ring, could potentially lower the thermodynamic barrier for flavin reduction (*17, 20*). The positive redox potential shifts presented in Table 1 are consistent with this model of polarization.

Scheme 1

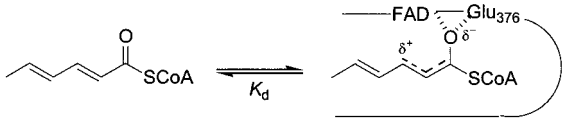

It is highly probable that the hydrogen bonds from the amide nitrogen of Glu376 and the 2′-hydroxy group of FAD play a major role in the polarization of HD-CoA. Similar interactions are of prime importance in causing selective ground-state polarization of HD-CoA in wild-type and mutant enoyl-CoA hydratase (*28*). While these hydrogen bonds will stabilize the accumulation of negative charge on the carbonyl oxygen (*20, 48*), additional electrostatic interactions with the hexadienoyl chain might be expected, to account for the *preferential* stabilization of a partial positive charge on carbon 3 (Scheme 1). Comparison of Raman data for HD-CoA bound to oxidized and reduced MCAD indicates that reduction of the flavin does not cause a significant change in the wavenumber of the normal mode associated with the hexadienoyl C(3)═C(2)−C(1)═O group (1568 vs 1567 cm^{-1}). This is consistent with positive charge developing at the C(3)−H region regardless of the oxidation state of the enzyme. Thus, the enzyme-induced polarization of the ligand likely does not involve strong electrostatic interactions between the flavin and the ligand. Consequently, the enzyme−ligand interactions responsible for the selective polarization of the ligand, other than the hydrogen bonds to the carbonyl group, remain to be identified.

It is also important to recognize that the size and electronic structure of the analogue itself can affect the way that it is polarized. Recent evidence obtained by Rudik and colleagues (*14*) suggests that binding may not disrupt π-electron conjugation in thioester product analogues containing phenol ring substituents. The pK_a of the phenol group of 4-hydroxycinnamoyl-CoA is lowered from 8.9 to 7.8 upon binding to E99G/E376Q human MCAD double mutant (*14*), indicating that polarization induced by the H-bonds to the thioester carbonyl is transmitted to the phenol ring system. If MCAD disrupted conjugation such that only the C(3)═C(2)−C(1)═O region was polarized, a pK_a shift for the phenoyl group would not be expected. Similar conclusions were drawn by Vock et al. (*11*) using *p*-NO_2-phenylacetyl-CoA as a ligand.

Currently there are no reports of enzyme ionization constants determined for actual substrate binding to MCAD. α-Proton abstraction by Glu376 prevents accurate measurement of this residue's pK_a when the oxidized enzyme is associated with true substrates. However, before α-proton abstraction occurs, pK_a shifts similar to those caused by HD-CoA binding are likely. Scheme 2 illustrates some of the pK_a and electron density changes proposed to result from the binding and oxidation of octanoyl-CoA. Proton transfer is shown for the system at pH 7.6 with shaded circles representing water molecules.

Both Glu99 and Glu376 are deprotonated in the oxidized, uncomplexed enzyme. Upon substrate binding (step 1), the

Scheme 2

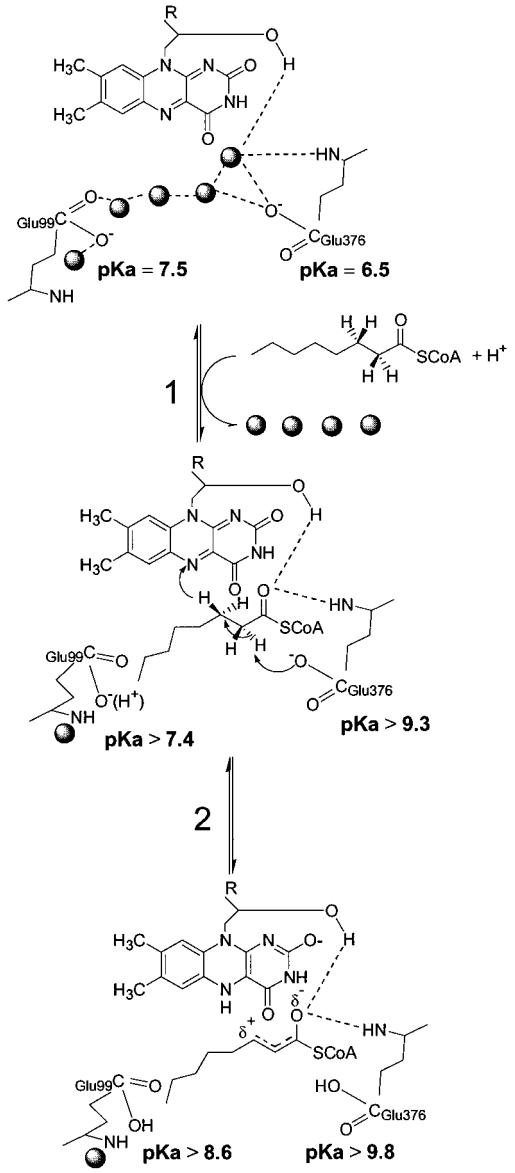

active site is almost completely desolvated, causing the pK_a of Glu376 and possibly the pK_a of Glu99 to be raised. Formation of an H-bond network with the thioester carbonyl lowers the pK_a of the αC−H bond from ≈21 (*9*), to between 8 and 12 (*11, 17, 48*−*50*). At this point, the α-proton can be abstracted by Glu376 and the *β*-hydride transferred to N(5) of the flavin (step 2), leaving a polarized resonance form of the *trans*-2-octenoyl-CoA product in complex with reduced MCAD. At pH 7.6, the reduced flavin is stabilized in the anionic form [pK_a for N(1) ≈ 6.9]. Propagation of this negative charge through the active site is likely to further suppress the ionization of Glu99 and Glu376, causing pK_a increases beyond what is attributed to desolvation. However, as noted earlier, the pK_a shift of Glu376 observed upon reduction of the flavin in the MCAD·HD-CoA complex is not as large as it is for free MCAD (1.9 vs 2.8 units). Possibly, the partial positive charge stabilized on C(3) compensates for some of negative charge developing on the FAD such that net negative charge felt by Glu376 is somewhat diminished. Consequently, the pK_a of Glu376 in the complex would not shift as much upon reduction as it does in the uncomplexed enzyme. This same argument may not apply to Glu99 as the distance between this residue and the substrate C(3) (≈8 Å) would limit the influence of positive charge on ionization of this glutamic acid (*17*). Using 3-thiaoctanoyl-CoA as an analogue, Vock et al. (*11*) have shown that the protonation state of Glu99 only affects ionization of the ligand αC−H when charge is allowed to delocalize beyond C(3). This is unlikely to occur with natural products that are selectively polarized. In any event, the ionization constants are sufficiently large such that both Glu376 and Glu99 should be protonated in the CT complex at pH 7.6.

CONCLUSION

The electrochemical and Raman studies of the MCAD·HD-CoA complex provide additional support for mechanistic hypotheses that include raising the pK_a of a catalytic base by substrate/product binding (*10, 11*) as well as product polarization (*10, 13, 19, 50*). Furthermore, these studies reveal that the polarization is carefully controlled such that an electron-deficient region is formed on the ligand, near the FAD isoalloxazine ring. As a result, the energy barrier for two-electron reduction of the FAD is lowered considerably (+93 mV, pH 7.6). It will be of interest in the future to identify and characterize the specific enzyme−ligand interactions that lead to this selective polarization.

ACKNOWLEDGMENT

We are grateful to Dr. Vernon Anderson for providing hexadienoyl-CoA and to Dr. Paul Carey for allowing use of his Raman instrument for initial experiments. We also thank Dr. Maurice Kreevoy for helpful discussions regarding hydrogen-bond-induced polarization.

REFERENCES

1. Thorpe, C., Matthews, R. G., and Williams, C., Jr. (1979) *Biochemistry 18*, 331−337.
2. Beinert, H. (1963) *Enzymes (2nd Ed.) 7*, 447−466.
3. Ghisla, S., Thorpe, C., and Massey, V. (1984) *Biochemistry 23*, 3154−3161.
4. Frerman, F. E., Miziorko, H. M., and Beckman, J. D. (1980) *J. Biol. Chem. 255*, 11192−11198.
5. Powell, P. J., and Thorpe, C. (1988) *Biochemistry 27*, 8022−8028.
6. Gorelick, R. J., Schopfer, L., Ballou, D. P., Massey, V., and Thorpe, C. (1985) *Biochemistry 24*, 6830−6839.
7. Thorpe, C. (1991) in *Chemistry and Biochemistry of Flavoenzymes* (Muller, F., Ed.) Vol. II, pp 471−486, CRC Press, Boca Raton, FL.
8. Johnson, B. D., and Stankovich, M. T. (1993) *Biochemistry 32*, 10779−10785.
9. Trievel, R. C., Wang, R., Anderson, V. E., and Thorpe, C. (1995) *Biochemistry 34*, 8597−8605.
10. Rudik, I., Ghisla, S., and Thorpe, C. (1998) *Biochemistry 37*, 8437−8445.
11. Vock, P., Engst, S., Elder, M., and Ghisla, S. (1998) *Biochemistry 37*, 1848−1860.
12. Mancini-Samuelson, G. J., Kieweg, V., Sabaj, K. M., Ghisla, S., and Stankovich, M. T. (1998) *Biochemistry 32*, 14605−14612.
13. Tamaoki, H., Nishina, Y., Shiga, K., and Miura, R. (1999) *J. Biochem. (Tokyo) 125*, 285−296.
14. Rudik, I., Bell, A. F., Tonge, P. J., and Thorpe, C. (2000) *Biochemistry 39*, 92−101.
15. Lenn, N. D., Stankovich, M. T., and Liu, H. (1990) *Biochemistry 29*, 3709−3715.

16. Bross, P., Engst, S., Strauss, A. W., Kelly, D. P., Rasched, I., and Ghisla, S. (1990) *J. Biol. Chem. 265*, 7116−7119.
17. Kim, J.-J. P., Wang, M., and Pashke, R. (1993) *Proc. Natl. Acad. Sci. U.S.A. 90*, 7523−7527.
18. Becker, D. F., Fuchs, J. A., Banfield, D. K., and Stankovich, M. T. (1993) *Biochemistry 32*, 10736−10742.
19. Becker, D. F., Fuchs, J. A., and Stankovich, M. T. (1994) *Biochemistry 33*, 7082−7087.
20. Johnson, B. D., Mancini-Samuelson, G. J., and Stankovich, M. T. (1995) *Biochemistry 34*, 7047−7055.
21. Nishina, Y., Sato, K., Hazekawa, I., and Shiga, K. (1995) *J. Biochem. 117*, 800−808.
22. Nishina, Y., Sato, K., Shiga, K., Fujii, S., Kuroda, K., and Miura, R. (1992) *J. Biochem. (Tokyo) 111*, 699−706.
23. Tonge, P. J., Anderson, V. E. Fausto, R., Kim, M., Pusztai-Carey, M., and Carey, P. R. (1995) *Biospectroscopy 1*, 387−394.
24. Kim, M., Owen, H., and Carey, P. R. (1993) *Appl. Spectrosc. 47*, 1780−1783.
25. Clarkson, J., Tonge, P. J., Taylor, K. L., Dunaway-Mariano, D., and Carey, P. R. (1997) *Biochemistry 36*, 10192−10199.
26. Lau, S. M., Powell, P., Buettner, H., Ghisla, S., and Thorpe, C. (1986) *Biochemistry 25*, 4184−4189.
27. Lenn, N. D. (1990) M.S. Thesis, University of Minnesota, Minneapolis, MN.
28. Bell, A. F., Wu, J., Feng, Y., and Tonge, P. J. (2000) *Biochemistry* (submitted for publication).
29. McIlwain, H. (1937) *J. Chem. Soc. 2*, 1704−1711.
30. Wu, W.-J., Anderson, V. E., Raleigh, D. P., and Tonge, P. J. (1997) *Biochemistry 36*, 2211−2220.
31. Pace, C. P., and Stankovich, M. T. (1994) *Arch. Biochem. Biophys. 331*, 261−266.
32. Stankovich, M. T. (1980) *Anal. Biochem. 109*, 295−308.
33. Stankovich, M. T., and Fox, B. (1983) *Biochemistry 22*, 4466−4472.
34. Einarsdotter, G. H., Stankovich, M. T., and Tu, S. C. (1988) *Biochemistry 27*, 3277−3285.
35. Clark, W. M. (1960) in *Oxidation−Reduction Potentials of Organic Systems*, Williams and Wilkins, New York.
36. O'Reilly, J. E. (1973) *Biochem. Biophys. Acta 292*, 509−515.
37. Johnson, B. D. (1993) Ph.D. Thesis, University of Minnesota, Minneapolis, MN.
38. Schopfer, L. M., Massey, V., Ghisla, S., and Thorpe, C. (1988) *Biochemistry 27*, 6599−6611.
39. Powell, P. J., Lau, S.-M., Killian, D., and Thorpe, C. (1987) *Biochemistry 26*, 3704−3710.
40. Peterson, K. L., Sergienko, E. E., Wu, Y., Kumar, N. R., Strauss, A. W., Oleson, A. E., Muhonen, W. W., Shabb, J. B., and Srivastava, D. K. (1995) *Biochemistry 34*, 14942−14953.
41. Niu, L. (1990) Ph.D. Thesis, University of Wisconsin, Madison, WI.
42. Morris, M. D., and Bienstock, R. J. (1986) in *Spectroscopy of Biological Systems* (Clark, R. J. H., and Hester, R. E., Eds.) Vol. 13, pp 395−442, Wiley, Chichester, U.K.
43. Hazekawe, I., Nishina, Y., Sato, K., Shichiri, M., Miura, R., and Shiga, K. (1997) *J. Biochem. (Tokyo) 121*, 1147−1154.
44. Nishina, Y., Sato, K., Miura, R., Matsui, K., and Shiga, K. (1988) *J. Biochem. (Tokyo) 124*, 200−208.
45. Tegoni, M., Gervais, M., and Desbois, A. (1997) *Biochemistry 36*, 8932−8946.
46. Kim, J.-J., Wang, M., Djordjevic, S., Paschke, R., Bennett, D. W., and Vockley, J. (1993) in *Flavins and Flavoproteins* (Yagi, K., Ed.) Vol. 376, pp 273−282, Walter de Gruyter and Co., Berlin.
47. Thorpe, C., and Kim, J.-J. P. (1995) *FASEB J. 9*, 718−725.
48. Gerlt, J. A., and Gassman, P. G. (1992) *J. Am. Chem. Soc. 114*, 5928−5934.
49. Shan, S., and Herschlag, D. (1996) *Proc. Natl. Acad. Sci. U.S.A. 93*, 14474−14479.
50. Engst, S., Vock, P., Wang, M., Kim, J.-J., and Ghisla, S. (1999) *Biochemistry 38*, 257−267.

BI0006464